Supplementary Information for

Boosting the electrochromic performance of P-doped WO_3 films via electrodeposition for smart window applications

Hongxi Gu*, Mengdi Tan, Ting Wang, Jiayi Sun, Juan Du*, Rong Ma, Wei Wang, Dengwei Hu

* Corresponding author

Engineering Research Center for Titanium Based Functional Materials and Devices in Universities of Shaanxi Province, Faculty of Chemistry and Chemical Engineering, Baoji University of Arts and Sciences, Baoji 721013 Shaanxi, China. *E-mail: hello1207@163.com, bwldj2010@163.com*

Characterization

The structural characterizations of the P-doped WO_3 films were analyzed by using a scanning electron microscope (SEM, FEI--Quanta 250 FEG) and transmission electron microscopy (JEOL JEM 2100F, 200 and 297 kV, JEOL Ltd., Tokyo, Japan). The crystal structures of the P-doped WO_3 films were evaluated by X-ray diffraction (XRD, Bruker D2 Phaser, Bruker D8, Karlsruhe, Germany) with Cu Kα radiation (λ = 1.5418 Å) in the 2θ range of 5−90°. The surface chemical state of the P-doped WO_3 films was checked using a NEXSA X-ray photoelectron spectrometer (Thermo Fisher Scientific, East Grinstead, UK) equipped with a monochromatic Al-Kα X-ray source (1486.6 eV). Acquisition parameters of high energy resolution photopeaks were 400-μm spot size, 12-kV primary energy, 6.0-mA emission intensity (corresponding to an irradiation power of 72 W), constant analyzer energy mode (CAE) 100 eV with 0.1-eV energy step size. The spectroelectrochemical measurement of the P-doped WO_3 films and the electrochromic devices were performed using a UV−vis−NIR spectrophotometer (U-4100, Hitachi, Tokyo, Japan). The electrochemical and electrochromic measurements were conducted in a three-electrode electrochemical cell containing 1 mol/L PC/$LiClO_4$ aqueous

solution as the electrolyte. Ag/AgCl as a reference electrode, and Pt wires as a counter electrode. Cyclic Voltammetry (CV) was performed at different scan rates (20, 40, 60, 80, and 100 mV/s) in the voltage range of -1 V to 1 V. The optical properties of the electrochromic devices were studied by using a UV-vis spectrophotometer with 10 simultaneous chronoamperometry (CA) cycles, 100 s for coloring (-1.0 V) and 100 s for bleaching (1.0 V). In addition, 600 cycles were performed under the same conditions for long-term stability assessment. EIS measurement was conducted by applying an AC voltage of 5mV over a frequency range of 10 Hz to 100 kHz. The spectroelectrochemical measurement of the ECD was applied at different potentials (1 V 100 s, -2.7 V 100 s). The solar-heat regulation test was carried out by a xenon lamp source (Solar-500, Beijing Newbit Technology Co., Ltd., Beijing, China).

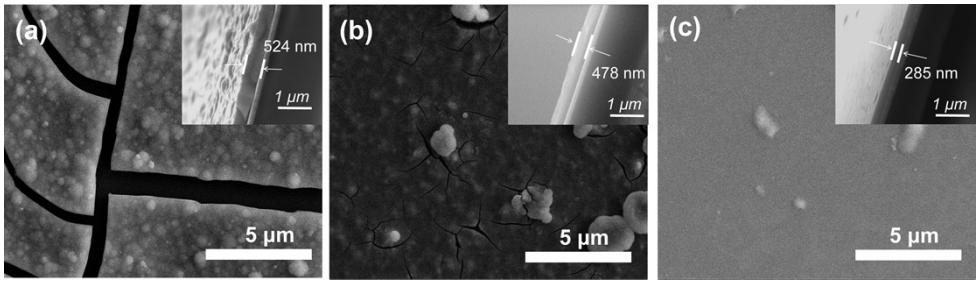

Fig. S1 SEM images of (a) PW-1 film, (b) PW-3 film, and (c) PW-4 films. (d) (insets: cross-sectional SEM images of the P-doped amorphous WO_3 films).

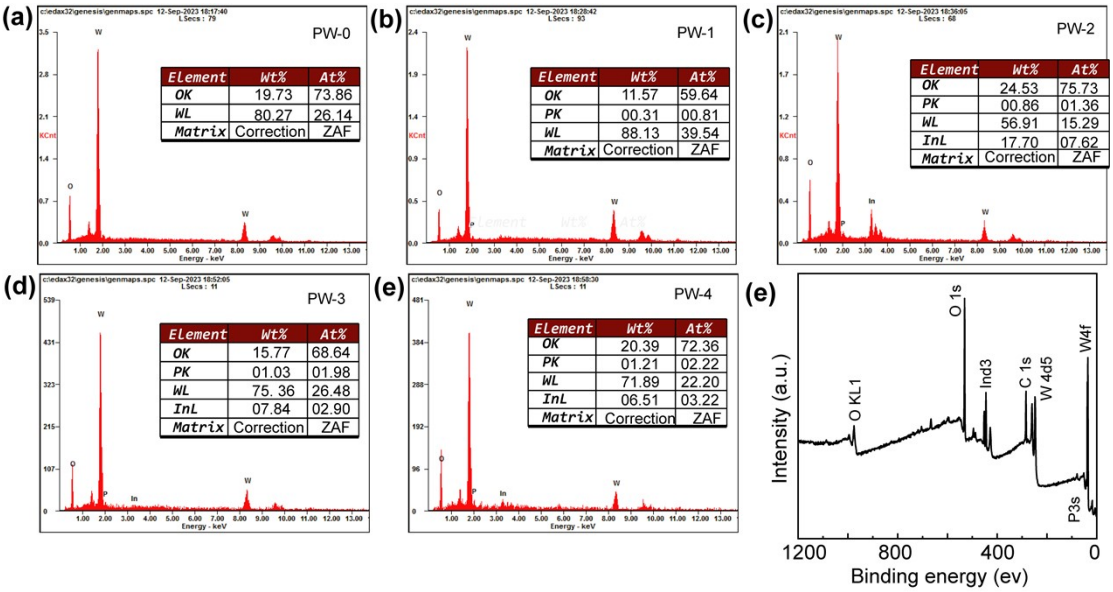

Fig.S2 EDX spectra of (a) PW-0 film, (b) PW-1 film (c) PW-2 film (d) PW-3 film, and (e) PW-4 film, (e) XPS spectra showing a full scan of the PW-2 film.

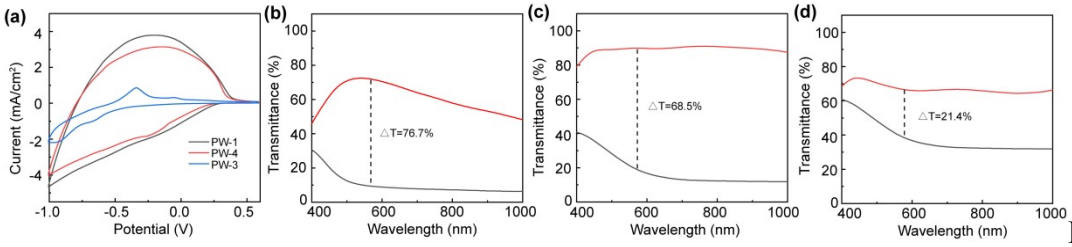

Fig.S3 (a) Cyclic voltammograms of the P-doped amorphous WO_3 films at a scan rate of 60 mV s^{-1} in 1 M PC/$LiClO_4$. Transmittance spectra of the (b) PW-1 film, (c) PW-3 film, and (d) PW-4 film in colored state at -1 V and bleached state at 1 V.

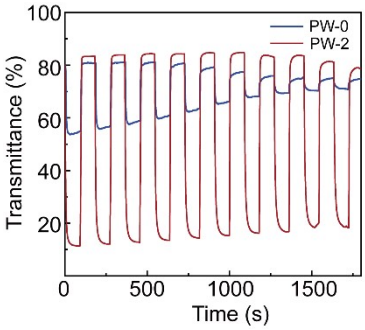

Fig.S4 In situ optical responses of the P-doped amorphous WO_3 films between the colored and bleached states for 100 s per step measured at 550 nm for 1800 s.

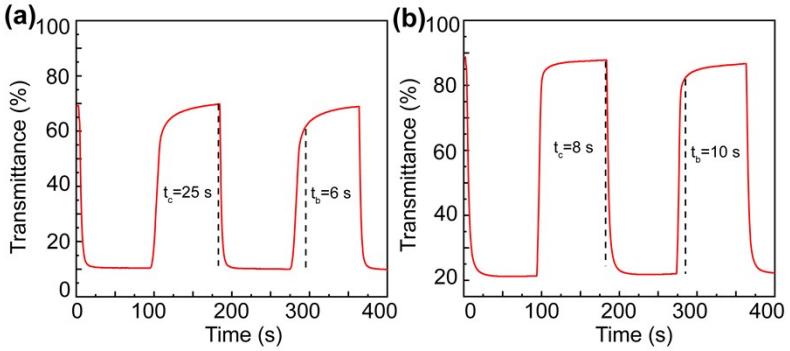

Fig. S5 The response times of the (a) PW-1 film and (b) PW-3 film.

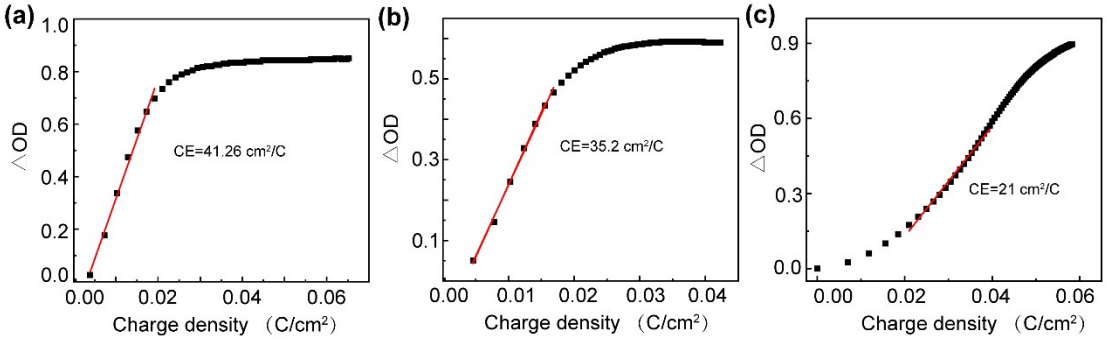

Fig. S6 Optical density *vs* the charge density of the (a) PW-1 film, (b) PW-3 film, and (c) PW-4 film at 550 nm with a potential of -1.0 V.

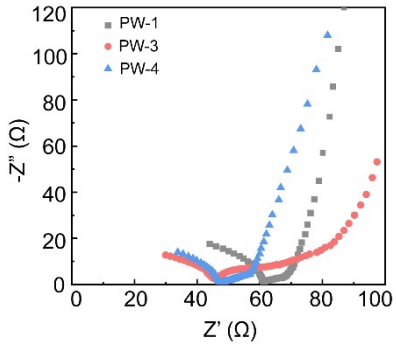

Fig. S7 Nyquist diagrams of the P-doped amorphous WO_3 films at the frequency of 10 Hz to 10^5 Hz.

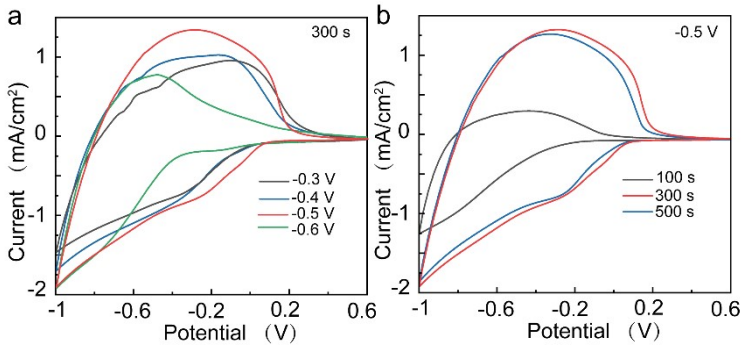

Fig.S8 Cyclic voltammograms of the PW-0 films at a scan rate of 60 mV s^{-1} in 1 M $PC/LiClO_4$. (a) under the same deposition time (300 s) (b) under the same deposition potential (-0.5 V)

Table S1 The electrochromic performance of PW-2 film compared with previous reports.

Material	Coloration time (s)	Bleaching time (s)	Optical contrast (%)	Coloration efficiency (cm^2 C^{-1})	Ref.
WO_3/AgNW	2	12	62.52	45.3	1
P-doped WO_3	6.1	2.5	55.8	55.9	2
Porous $WO_3 \cdot 2H_2O$ film	4.7	12.8	75.6	178.8	3
WO_3-PB	18	30	66.22	137.8	4
WO_3:Mo	26	36	57.5	67.58	5
Sol-gel WO_3	31.72	9.58	40	34.8	6
WO_3-Au/PEDOT/Pt	25.86	15.93	21.9	/	7
This work	6	8	80.9	53	

Reference

[1] Y.-T. Park, S.-H. Lee, K.-T. Lee, Electrochromic properties of silver nanowire-embedded tungsten trioxide thin films fabricated by electrodeposition, Ceram. Int. 46(18) (2020) 29052-29059.

[2] K. Bon-Ryul, K.-H. Kim, H.-J. Ahn, Novel tunneled phosphorus-doped WO_3 films achieved using ignited red phosphorus for stable and fast switching electrochromic

performances, Nanoscale. 11(7) (2019) 3318-3325.

[3] Z. Zhou, Z. Chen, D. Ma, J. Wang, Porous $WO_3 \cdot 2H_2O$ film with large optical modulation and high coloration efficiency for electrochromic smart window, Sol. Energ. Mat. Sol. C. 253 (2023) 112226-112234.

[4] H. Li, C.J. Firby, A.Y. Elezzabi, Rechargeable Aqueous Hybrid Zn^{2+}/Al^{3+} Electrochromic Batteries, Joule. 3(9) (2019) 2268-2278.

[5] E. Eren, G.Y. Karaca, U. Koc, L. Oksuz, A.U. Oksuz, Electrochromic characteristics of radio frequency plasma sputtered WO_3 thin films onto flexible polyethylene terephthalate substrate, Thin Solid Films, 634 (2017) 40–50.

[6] B.W.-C. Au, K.-Y. Chan, D. Knipp, Effect of film thickness on electrochromic performance of sol-gel deposited tungsten oxide (WO_3), Opt. Mater. 94 (2019) 387–392.

[7] G.Y. Karaca, E. Eren, G.C. Cogal, E. Uygun, L. Oksuz, A.U. Oksuz, Enhanced electrochromic characteristics induced by Au/PEDOT/Pt microtubes in WO_3 based electrochromic devices, Opt. Mater. 88 (2019) 472–478.